



Improved circuit model for left-handed lines loaded with split ring resonators

F. Aznar, J. Bonache, and F. Martín

Citation: [Applied Physics Letters](#) **92**, 043512 (2008); doi: 10.1063/1.2839600

View online: <http://dx.doi.org/10.1063/1.2839600>

View Table of Contents: <http://scitation.aip.org/content/aip/journal/apl/92/4?ver=pdfcov>

Published by the [AIP Publishing](#)



Re-register for Table of Content Alerts

Create a profile.



Sign up today!



Improved circuit model for left-handed lines loaded with split ring resonators

F. Aznar,^{a)} J. Bonache, and F. Martín^{b)}

CIMITEC, Departament d'Enginyeria Electrònica, Universitat Autònoma de Barcelona, Bellaterra, 08193 Barcelona, Spain

(Received 17 December 2007; accepted 12 January 2008; published online 1 February 2008)

In this letter, an improved lumped element equivalent circuit model for left-handed lines based on split ring resonators (SRRs) is presented and discussed. It is rigorously demonstrated that although the previously accepted circuit model of these metamaterial transmission lines (a π circuit) provides a good description of device behavior, its electrical parameters do not actually describe the physics of the structure. Conversely, the parameters of the improved equivalent circuit model are representative of the different elements of the structure, including the SRRs, the shunt inductive elements and the host line. It is also shown that the proposed model can be transformed to a π model which is formally identical to the previous reported model of SRR-based left-handed lines. With this transformation, the main relevant characteristics of these left-handed lines are perfectly interpreted. © 2008 American Institute of Physics. [DOI: 10.1063/1.2839600]

Resonant-type metamaterial transmission lines were proposed by Martín *et al.*¹ in 2003 by loading a coplanar waveguide (CPW) structure with split ring resonators (SRRs).² Such resonators, consisting on a pair of concentric metallic rings with slits etched on opposite sides, are electrically small³ and were formerly used in 2000 by Smith *et al.*⁴ for the synthesis of a bulk left-handed medium. Indeed, the left-handed SRR-based CPW reported in Ref. 1 was inspired on the medium of Smith *et al.*⁴ By etching SRRs in the back substrate side, beneath the slots, and shunt connected metallic strips between the central strip and ground plane, a one-dimensional effective medium with simultaneous negative permeability (due to the presence of the SRRs) and permittivity (thanks to the shunt strips) in a narrow band was achieved.¹ It was also demonstrated^{1,5} that by removing the shunt connected strips of the structure, a stop-band characteristic is obtained, and this was interpreted as due to the negative and highly positive effective permeability of the structure above and below SRR's resonance, respectively.

Alternatively, the behavior of these SRR-based structures (with and without shunt connected strips) can be interpreted to the light of the lumped element equivalent circuit models of the unit cells, which were reported in Ref. 1 and are reproduced here for completeness (see Fig. 1). As was reported in Ref. 1, L and C account for the line inductance and capacitance, respectively, C_s and L_s model the SRR, M is the mutual inductive coupling between the line and the SRRs, and L_p is the inductance of the shunt strips. In the models of Fig. 1, the magnetic wall concept has been used. From the transmission line approach of metamaterials,^{6,7} it follows that the structure exhibits left-handed wave propagation in those regions where the series reactance and shunt susceptance are negative, whereas the requirement for an effective medium with negative permeability is a negative series reactance and a positive shunt susceptance. According to this, the models of Fig. 1 perfectly explain the propagation

characteristics of the structures. However, the unit cell model of the left-handed structure is not able to accurately describe its behavior. The reasons are investigated in this paper, where we propose an improved model which can be transformed to that of Fig. 1(c) with modified parameters.

According to the π -circuit models of Fig. 1, the structures should exhibit a transmission zero (all injected power is returned back to the source) at that frequency ω_z , where the series branch opens [$Z_s(\omega_z)=\infty$, where $Z_s(\omega)$ is the impedance of the series branch], and it occurs at the resonance frequency of the SRRs ω_0 for both circuit models. In other words, the transmission zero should be located at identical frequency (provided identical SRRs are used) in both structures (with and without shunt strips). Moreover, according to the models of Fig. 1, the allowed band in the left-handed CPW structure should be slightly shifted toward positive values as compared to the stop band in the negative-permeability line (structure without shunt strips). This is due

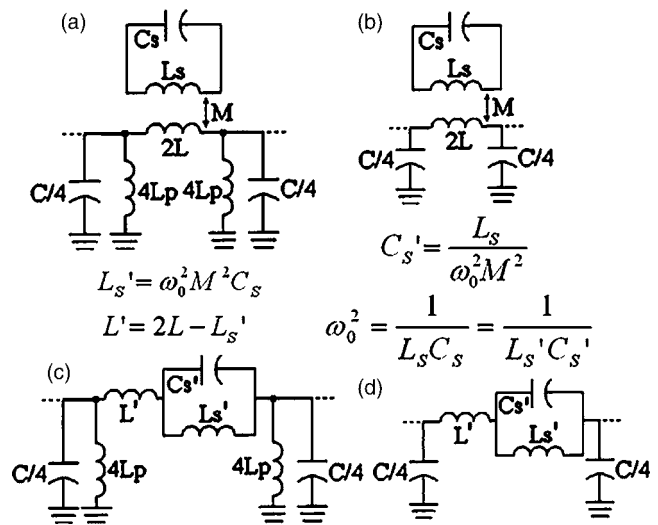


FIG. 1. Lumped element equivalent circuit for the basic cell of the left-handed (a) and negative-permeability (b) CPW structures loaded with SRRs. These circuits can be transformed to those depicted in (c) and (d), according to the indicated transformations.

^{a)}Electronic mail: francisco.aznar@uab.es.
^{b)}Tel.: 34935813522. Fax: 34935812600.
 Electronic mail: ferran.martin@uab.es.

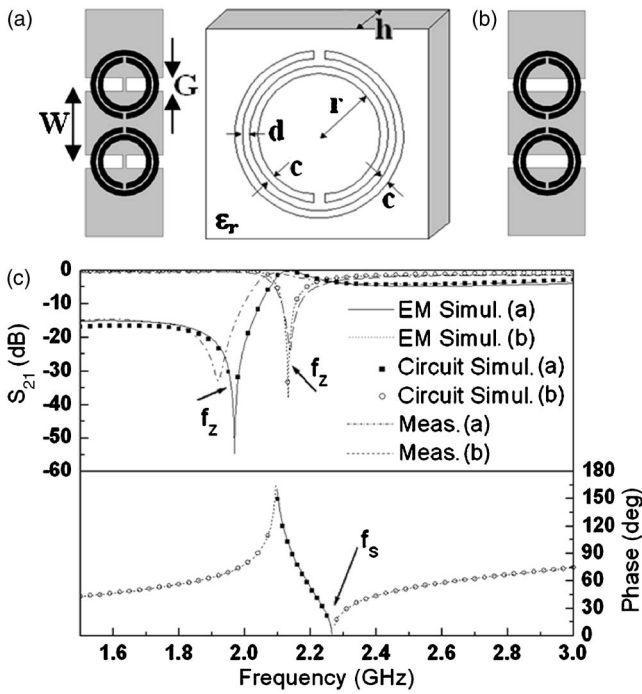


FIG. 2. Layout of the considered CPW structures with SRRs and shunt strips (a) and with SRRs only (b); simulated and measured transmission coefficient S_{21} and simulated dispersion relation (c). The considered substrate is the Rogers RO3010 with thickness $h=1.27$ mm and dielectric constant $\epsilon_r=10.2$. Relevant dimensions are rings width $c=0.6$ mm, distance between the rings $d=0.2$ mm, and internal radius $r=2.4$ mm. For the CPW structure, the central strip width is $W=7$ mm and the width of the slots is $G=1.35$ mm. Finally, the shunt strip width is 0.2 mm. The results of the electrical simulation with extracted parameters are depicted by using symbols. We have actually represented the modulus of the phase since it is negative for the left-handed line. Discrepancy between measurement and simulation for circuit (a) is attributed to fabrication related tolerances.

to the fact that the left-handed band is located to the right of $\omega_0=\omega_z$, whereas the stop band extends below and above ω_0 , as has been explained above. In the negative-permeability and left-handed CPW structures reported in Ref. 1, these features apparently occur. However, these structures are composed of four cascaded unit cells, and this may obscure device behavior. Namely, to better identify the position of the transmission zero and the allowed band (left-handed structure), it is convenient to consider a single unit cell line. Under these conditions, the transmission zero is not obscured by surface waves, and the transmission peak in the left-handed structure can be easily identified since the effects of losses are minimized. Thus, we have considered two identical single cell structures, one with shunt strips, the other one without shunt strips (Fig. 2). The transmission (S_{21}) and reflection (S_{11}) coefficients of these structures have been obtained from full wave electromagnetic simulation using the AGILENT MOMENTUM commercial software. We have also obtained the dispersion relation of this structure, following the standard procedure:

$$\cos(\beta l) = \frac{A + D}{2}, \tag{1}$$

where β is the phase constant, l is the unit cell length, and A and D are the diagonal elements of the transmission ($ABCD$) matrix, which can be inferred from the simulated reflection and transmission coefficients.⁸ These results are depicted in Fig. 2. Two relevant characteristics are readily visible: (i) the

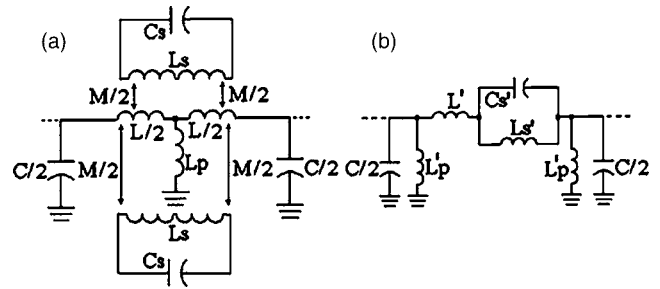


FIG. 3. Proposed improved circuit model for the basic cell of the left handed CPW structure (a). Transformation of the model to a π circuit (b), according to the procedure described in the text.

transmission zero is shifted toward negative values in the left-handed line, as compared to the negative-permeability line, and (ii) the phase shift, $\phi=\beta l$, nulls at identical frequency in both structures. From the π -circuit model, the dispersion diagram can be inferred as follows:

$$\cos(\beta l) = 1 + \frac{Z_s(\omega)}{Z_p(\omega)}, \tag{2}$$

where $Z_s(\omega)$ and $Z_p(\omega)$ are the series and shunt impedances of the π -circuit model. According to the results of Fig. 2, the models of Fig. 1 cannot be both correct since they predict identical transmission zero frequency. Thus, we must assume that at least one of the π circuits shown in Fig. 1 is incorrect, as it is. Specifically, the series branch must be different in order to explain the different values of the transmission zero frequency. However, surprisingly, in spite of the different series impedances, these impedances must null at identical frequency, since $\phi=0$ when $Z_s(\omega)=0$ (the left-handed and negative-permeability structures exhibit zero-degree phase shift at the same frequency).

As will be shown, this phenomenology can perfectly be explained by considering an improved circuit model for the left-handed line (leaving the circuit model of the negative-permeability structure unaltered). This is depicted in Fig. 3(a) (the magnetic wall concept is not considered since this is not actually necessary). In this model, the reactive parameters have the same interpretation, as in the models of Fig. 1. However, the inductance of the shunt inductive strips L_p is now located between the two inductances ($L/2$) that model each line section, to the left and right of the position of the shunt strips. This improved model reflects the location of the inductive strips, as was reported in Ref. 9. The model is neither a π circuit nor a T circuit. Thus, the transmission zero frequency and the frequency where the phase shift nulls cannot be directly obtained from it. The main relevant aspect of this letter is to demonstrate that the model of Fig. 3(a) can be transformed to a π circuit, formally identical to that of Fig. 1(c) with modified parameters. From this transformation, the shift of the transmission zero toward lower frequencies as compared to the structure without shunt strips, and the preservation of the frequency where $\phi=0$, can perfectly be explained.

Due to symmetry considerations and reciprocity, the admittance matrix of the circuit of Fig. 3(a) (which is a biport) must satisfy $Y_{12}=Y_{21}$ and $Y_{11}=Y_{22}$. From these matrix elements, the equivalent π -circuit model can be obtained according to Ref. 8.

$$Z_s(\omega) = -(Y_{21})^{-1}, \quad Z_p(\omega) = (Y_{11} + Y_{21})^{-1}. \quad (3)$$

Y_{21} is inferred by grounding port 1 and obtaining the ratio between the current at port 1 and the applied voltage at port 2. Y_{11} is simply the input admittance of the biport, seen from port 1, with a short circuit at port 2. After a straightforward but tedious calculation, the elements of the admittance matrix are obtained, and by applying Eqs. (3), we finally obtain

$$Z_s(\omega) = j\omega \left(2 + \frac{L}{2L_p} \right) \left[\frac{L}{2} + M^2 \frac{1 + \frac{L}{4L_p}}{L_s \left(\frac{\omega_0^2}{\omega^2} - 1 \right) - \frac{M^2}{2L_p}} \right], \quad (4a)$$

$$Z_p(\omega) = j\omega \left(2L_p + \frac{L}{2} \right), \quad (4b)$$

with $\omega_0 = (L_s C_s)^{-1/2}$. Expression (4a) can be rewritten as

$$Z_s(\omega) = j\omega \left(2 + \frac{L}{2L_p} \right) \left[\frac{L}{2} - L'_s + \frac{L'_s}{1 - L'_s C'_s \omega^2} \right], \quad (5)$$

with

$$L'_s = 2M^2 C_s \omega_0^2 \frac{\left(1 + \frac{L}{4L_p} \right)^2}{1 + \frac{M^2}{2L_p L_s}}, \quad C'_s = \frac{L_s}{2M^2 \omega_0^2} \left(\frac{1 + \frac{M^2}{2L_p L_s}}{1 + \frac{L}{4L_p}} \right)^2. \quad (6)$$

These results indicate that the improved circuit model of the unit cell of the left-handed lines loaded with SRRs and shunt inductors [Fig. 3(a)] can be formally expressed as the π circuit of Fig. 1(c), but with modified parameters [Fig. 3(b)]. This modified parameters are related to the parameters of the circuit of Fig. 3(a), according to Eqs. (6) and

$$L' = \left(2 + \frac{L}{2L_p} \right) \frac{L}{2} - L'_s, \quad L'_p = 2L_p + \frac{L}{2}. \quad (7)$$

The transmission zero frequency ω_z for the circuit of Fig. 3 is no longer given by the resonance frequency of the SRRs ω_0 , but it is smaller, that is, $\omega_z \ll \omega_0$. On the other hand, the frequency where $\phi=0$ ω_s is obtained by forcing $Z_s(\omega)=0$. This gives

$$\omega_s = \frac{1}{\sqrt{C_s \left(L_s - 2 \frac{M^2}{L} \right)}}. \quad (8)$$

Despite that $Z_s(\omega)$ is a function of L_p , unexpectedly, ω_s does not depend on the shunt inductance. This explains that ω_s is identical for both the left handed and negative-permeability structures.

This analysis reveals that the previous reported circuit model of left-handed lines loaded with SRRs and shunt inductive elements [Fig. 1(c)] is formally correct [it is formally identical to that of Fig. 3(b)]. The weakness relies on the physical interpretation of the elements of that model. It has been demonstrated in this letter that these elements [i.e., the elements of the circuit of Fig. 3(b)] do not have any physical meaning. However, they are related to the elements of the circuit model of Fig. 3(a), which describe the different components of the left-handed unit cell. To further confirm the validity of the proposed circuit model of left-handed lines

TABLE I. Extracted parameters for the SRR-loaded CPW unit cells with and without shunt strips, and estimated values (third row).

Shunt strips	L_p (nH)	C (pF)	L (nH)	M (nH)	L_s (nH)	C_s (pF)
Yes	0.36	2.44	2.17	1.18	11.23	0.50
No	...	2.44	2.21	1.20	11.22	0.50
Estimated	0.56	2.13	2.60	1.45	12.55	0.50

based on SRRs, we have considered two identical structures (unit cells), one with shunt connected strips (left-handed line), the other without these elements, and we have extracted the parameters of both structures (from the electromagnetic simulation) according to a procedure similar to that described in Ref. 10. The circuit of Fig. 3(b) has been considered for the left-handed unit cell, whereas for the structure without shunt strips, we have considered the circuit model that results by forcing $L_p = \infty$. The electrical simulation of both circuits is also depicted in Fig. 2 to ease the comparison with the electromagnetic simulation. The agreement is excellent. On the other hand, we have inverted Eqs. (6) and (7) in order to obtain the parameters of the model of Fig. 3(a), and they show a very good agreement with those parameters inferred in the structure without shunt strips (see Table I), which means that the presence of the shunt strip does not affect the parameters of the structure, hence having a clear physical interpretation. Alternatively, L_s and C_s can be inferred from the geometry of the SRRs by following the method reported in Ref. 7, L and C can be estimated from the dispersion relation and the characteristic impedance of the artificial line loaded with SRRs (i.e., without shunt strips) at low frequencies, and L_p can be obtained from independent full wave electromagnetic simulations of a zero-length CPW structure loaded with a pair of shunt strips (and modeled through a shunt inductance). The results are also given in Table I.

In conclusion, the previously existing and accepted models of SRR-loaded CPW metamaterial transmission lines have been revised. For SRR-loaded left-handed lines, some effects were found not to be explained by the former circuit model, and an improved model has been proposed and exhaustively analyzed. It has been concluded that the revised model can be transformed to a π circuit formally identical to that previously reported but with modified parameters.

¹F. Martín, F. Falcone, J. Bonache, R. Marqués, and M. Sorolla, *Appl. Phys. Lett.* **83**, 4652 (2003).

²J. B. Pendry, A. J. Holden, D. J. Robbins, and W. J. Stewart, *IEEE Trans. Microwave Theory Tech.* **47**, 2075 (1999).

³J. García-García, F. Martín, J. D. Baena, R. Maques, and L. Jelinek, *J. Appl. Phys.* **98**, 033103 (2005).

⁴D. R. Smith, W. J. Padilla, D. C. Vier, S. C. Nemat-Nasser, and S. Schultz, *Phys. Rev. Lett.* **84**, 4184 (2000).

⁵F. Martín, F. Falcone, J. Bonache, T. Lopetegi, R. Marqués, and M. Sorolla, *IEEE Microw. Wirel. Compon. Lett.* **13**, 511 (2003).

⁶C. Caloz and T. Itoh, *Electromagnetic Metamaterials: Transmission Line Theory and Microwave Applications* (Wiley, New Jersey, 2006).

⁷R. Marqués, F. Martín, and M. Sorolla, *Metamaterials with Negative Parameters: Theory, Design and Microwave Applications* (Wiley, New Jersey, 2008).

⁸M. Pozar, *Microwave Engineering* (Addison Wesley, New York, 1990).

⁹L. Roglá, J. Carbonell, and V. E. Boria, *IET Proc. Microwaves, Antennas Propag.* **1**, 170 (2007).

¹⁰J. Bonache, M. Gil, I. Gil, J. García-García, and F. Martín, *IEEE Microw. Wirel. Compon. Lett.* **16**, 543 (2006).